Sustainable Cities and Society 109 (2024) 105525

Contents lists available at ScienceDirect

Sustainable Cities and Society

journal homepage: www.elsevier.com/locate/scs

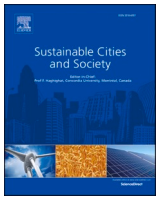

Beyond built environment: Unveiling the interplay of streetscape perceptions and cycling behavior

Jin Rui [a,*], Yuhan Xu [b]

[a] Department of Spatial Planning, Technical University Dortmund, August-Schmidt-Straße 10, 44227, Dortmund, Germany
[b] School of Architecture, Southeast University, 2 Sipailou, Nanjing, 210096, China

ARTICLE INFO

Keywords:
Street view images
Eye-level perceptions
Street environment
Bicycle-sharing behavior
Built environment

ABSTRACT

As an important means of shared micro-mobility, shared bicycles have become a crucial component of urban transportation in China. The impact of the built environment on bicycling has been widely acknowledged. However, can streetscape perceptions influence bicycle-sharing volume (BSV) and supplement the built environment? We first obtained millions of pieces of shared-cycling data from the Shenzhen Open Data Platform and carried out geographical quantification of BSV. As for streetscape, we improved the classification of subjective streetscape perception based on street view images using the k-means clustering algorithm and conducted predictions using XGBoost. Through the application of different regression models, we unveiled the nonlinear spatial interdependencies between BSV and streetscape perceptions as a complement to the built environment. Our findings indicate that greenery, vivid street-front facades, and diverse street facilities can promote BSV. Targeted strategies are proposed for different districts. For instance, urban planners can provide incentives for high-income groups in central urban areas to adopt active travel, and increase the supply of shared bicycles in suburban areas with high building density, particularly in industrial urban villages. As a supplement to the long-term planning recommendations derived from the macro-built environment analysis, an in-depth spatial perception quantitative assessment proffers a human-centric, flexible blueprint for urban street design.

1. Introduction

Chinese cities have placed excessive emphasis on the development of motorized traffic while neglecting the rights of non-motorized transportation during the urbanization process, leading to issues such as traffic congestion and high carbon emissions (Li et al., 2023; Su et al., 2022). One approach to alleviate these urban challenges is to encourage a shift towards low-carbon transportation modes. A novel concept in the transportation field that can mitigate this problem is Shared Micro-Mobility Services (SMS) (Huang et al., 2023; Lin et al., 2023; Wang & Zhang, 2023). SMS typically refers to shared, lightweight, low-speed, and eco-friendly modes of transportation such as shared bicycle systems (Gong et al., 2024; Tong et al., 2023). These methods have been proven to offer multiple benefits, including solving the problems of the "first mile" and "last mile," reducing reliance on private vehicles and their carbon emissions, and promoting physical activity among urban residents, thus helping to alleviate urban issues (Milakis et al., 2020; Pettersson et al., 2016). On the one hand, promoting shared micro-mobility can help reduce traffic congestion and accelerate the decarbonization of the transportation sector (Rui & Othengrafen, 2023). On the other hand, integrating walkways and bike lanes with public transportation systems can address the "last mile" problem (Rogers III et al., 2023). This approach is particularly promising in emerging areas of megacities, where the establishment of dedicated bicycle lanes can facilitate the creation of 15-minute city life circles, thereby improving the spatial accessibility and convenience for local residents.

In recent years, SMS has become one of the indispensable modes of transportation for in China. According to the "2022 Annual Report on Bicycle/Electric Bicycle Riding in Major Cities" (https://www.100ec.cn/index.php/detail–6619306.html), 77% of the rail transit stations are serviced by shared bicycles, with the average city serving nearly 80% of the commuting population. In Shenzhen, the population served by shared bicycle commuting accounts for over 90%. As per the "Urban Comprehensive Transportation System Planning Standards (GB/T 51328-2018)", shared bicycles have been integrated into public transport system. This provides a reliable data source for cycling behavior studies. Previous research derived travel behavior data from travel surveys, a method that proved to be time-consuming, labor-intensive,

* Corresponding author.
E-mail addresses: jin.rui@tu-dortmund.de (J. Rui), xuyh_seu@163.com (Y. Xu).

https://doi.org/10.1016/j.scs.2024.105525
Received 8 January 2024; Received in revised form 28 March 2024; Accepted 12 May 2024
Available online 20 May 2024

and constrained in spatiotemporal coverage. With the popularity of shared bicycles and the incorporation of GPS, the acquisition of millions of digital footprints has become possible, significantly expanding the spatiotemporal scale of the study of cycling behavior.

Streets accommodate all road users, and the quality of streets is closely linked to the travel mode choice of its residents (Kabisch et al., 2021; Kim et al., 2023; Rui & Othengrafen, 2023). Streets designed with cycling-friendly features can encourage cycling behavior among residents (Nawrath et al., 2019), and streets that are accessible, open, clean, safe, and offer natural scenery can attract more cyclists (Dong et al., 2023). There is a need for most Chinese cities to promote bicycle-friendly street environment. As of the end of 2019, Shenzhen boasts approximately 1759 km of bicycle traffic lanes, accounting for around 13.7% of the total road mileage. At the macro level, the low installation rate and inadequate quality of bicycle lanes, along with insufficient right-of-way and safety measures, pose significant obstacles to the development of bicycle transportation in Shenzhen. At the micro level, the complex relationship between street environments and bicycles requires further research to supplement existing studies on the built environment, in order to better carry out bottom-up, bicycle--friendly design.

With the emergence of advanced computational techniques, such as semantic segmentation, quantifying street environment features has become possible. By integrating spatiotemporal data from various sources, researches have achieved the "measurement of the unmeasurable" (Ewing & Handy, 2009), enabling large-scale, fine-grained street environment assessments (Dong et al., 2023; Rui, 2023b; Wang et al., 2022). Ito and Biljecki (2021) evaluated bikeability using street view images (SVIs) and computer vision, enhancing parameters such as connectivity, environmental quality, infrastructure by incorporating perceptual factors like aesthetics, safety, and cleanliness. Song et al. (2023) undertook a quantification of perceived indices—spanning order, accessibility, aesthetic value, ecological considerations, enclosure, richness, and scale—by sampling 300 SVIs at random, aiming to elucidate the effects of micro-environmental attributes on bicycle-sharing practices.

Current studies exhibit certain constraints. First, there is an absence of research that integrates both subjective and objective perceptions to offer bottom-up recommendations for designing bike-friendly streets. Second, the Place Pulse dataset for streetscape perception is not applicable to the Chinese urban landscape (Qiu et al., 2023; Wu et al., 2023; Zhang et al., 2018). Self-trained datasets have methodological shortcomings. For instance, the random selection of SVIs fails to capture features of all SVIs (Qiu et al., 2023). Variables such as "ecology" and "accessibility" not only transcend the conventional perception ambit but also pose significant quantification challenges when reliant solely on SVIs (Song et al., 2023). Third, studies often overlook the complex geographical and non-linear relationships between environmental variables and bicycle-sharing volume (BSV). Singular regression models struggle to comprehensively articulate intricate dependencies (Meng et al., 2016; Nawrath et al., 2019; Parkin et al., 2008; Spotswood et al., 2015).

The objective of our study is to elucidate the impact of visual streetscape perceptions on promoting BSV as a supplement to the built environment, providing bottom-up suggestions for promoting SMS and designing bicycle-friendly streets. Our study introduced three novel contributions that address identified research gaps: 1) By integrating a human-centric visual sampling approach, we achieved a holistic quantification of streetscape perceptions, spanning both objective and subjective aspects. 2) We created a comprehensive dataset emphasizing subjective streetscape perceptions based on Chinese urban landscapes. The application of the k-means clustering ensured the diversity of features in SVIs. 3) Our research delved into the intricate, nonlinear, and spatial dynamics between eye-level streetscape perceptions and BSV. The findings from perception study offer human-centered street design solutions, supplementing long-term planning recommendations derived from the built environment.

2. Data and methodology

2.1. Conceptual framework

Our conceptual framework is divided into four steps (Fig. 1). Initially, we extracted shared bicycle data, Baidu-SVIs, Points of Interest (POIs), and OpenStreetMap (OSM) road data. Secondly, we transformed the shared bicycle data into BSV to serve as the dependent variable. The data processing for SVIs encompassed two aspects: (a) the first entailed acquiring pixel-level information through semantic segmentation, facilitating the derivation of objective perceptual variables, and (b) utilizing K-means clustering algorithm, participant scoring, and machine prediction models to derive subjective streetscape perceptions. Moreover, the analysis of POI data and the road network within a GIS framework yielded the built environment (BE) attributes. Thirdly, we employed Moran's I test, Multiscale Geographically Weighted Regression (MGWR), and XGBoost models to conduct both geospatial and numerical analyses, engaging in a collaborative discussion of the findings. Fourthly, we identified priorities for crafting cyclist-friendly streets and proposed adaptive, human-centric recommendations for street renovations based on perceptual analysis.

2.2. Study area, street view image (SVI) collection and segmentation

Shenzhen is located in the southern part of Guangdong Province, China. The *Shenzhen Bicycle Transportation Development Plan (2021-2025)* (Shenzhen Transportation Department, 2021) reveals that the total daily travel volume in Shenzhen is approximately 43.78 million trips. Cycling accounts for 8.2% of the overall travel mode share, with shared bicycles contributing an average of 1.6083 million trips per day, representing about 3.7% of the total transportation share. Excluding electric bicycles, shared cycling makes up around 45% of all cycling activities. This indicates that shared bicycle trips are representative of bicycle travel in the city. We selected the primary areas of Shenzhen associated with the bicycle skeleton network and recreational paths, namely the six urban districts of Nanshan, Futian, Luohu, Bao'an, Longhua, and Guangming (Fig. 2.a). We focused on 481 communities that possess both existing streetscape data and shared bicycle riding statistics as our analytical units.

We established a sampling point every 50 meters on the street network, resulting in a total of 84,876 sampling points. We used the Baidu API interface to retrieve Baidu-SVI panoramic images for each sampling point (Fig. 2.b). During the data scraping process, we set the pitch to 20, the field of view (fov) to 360, and the heading to 0. Deeplab V3+ has been proven to be effective in the segmentation of SVIs (Rui, 2023b). Therefore, we employed Deeplab V3+ with pre-trained datasets ADE20K to perform semantic segmentation on SVIs. The results of the semantic segmentation primarily consisted of statistical tables detailing the proportions of different streetscape elements and the segmented SVIs (Fig. 2.c).

2.3. Data collection and processing

2.3.1. Dependent variable: bicycle-sharing volume (BSV)

The bicycle-sharing data was sourced from the Shenzhen Municipal Government Data Open Platform (https://opendata.sz.gov.cn/). Attributes of the data include start and end time with corresponding latitude and longitude. The study employed shared bicycle-sharing data from February 1st, 2021. The original dataset comprised 1,438,225 records, of which rides lasting more than one minute were deemed valid, resulting in 1,416,605 valid entries.

Given the extensive volume of the data, it was considered appropriate to associate the start and end points to the centroids of 500-meter hexagonal grids, followed by the generation of bicycle-sharing

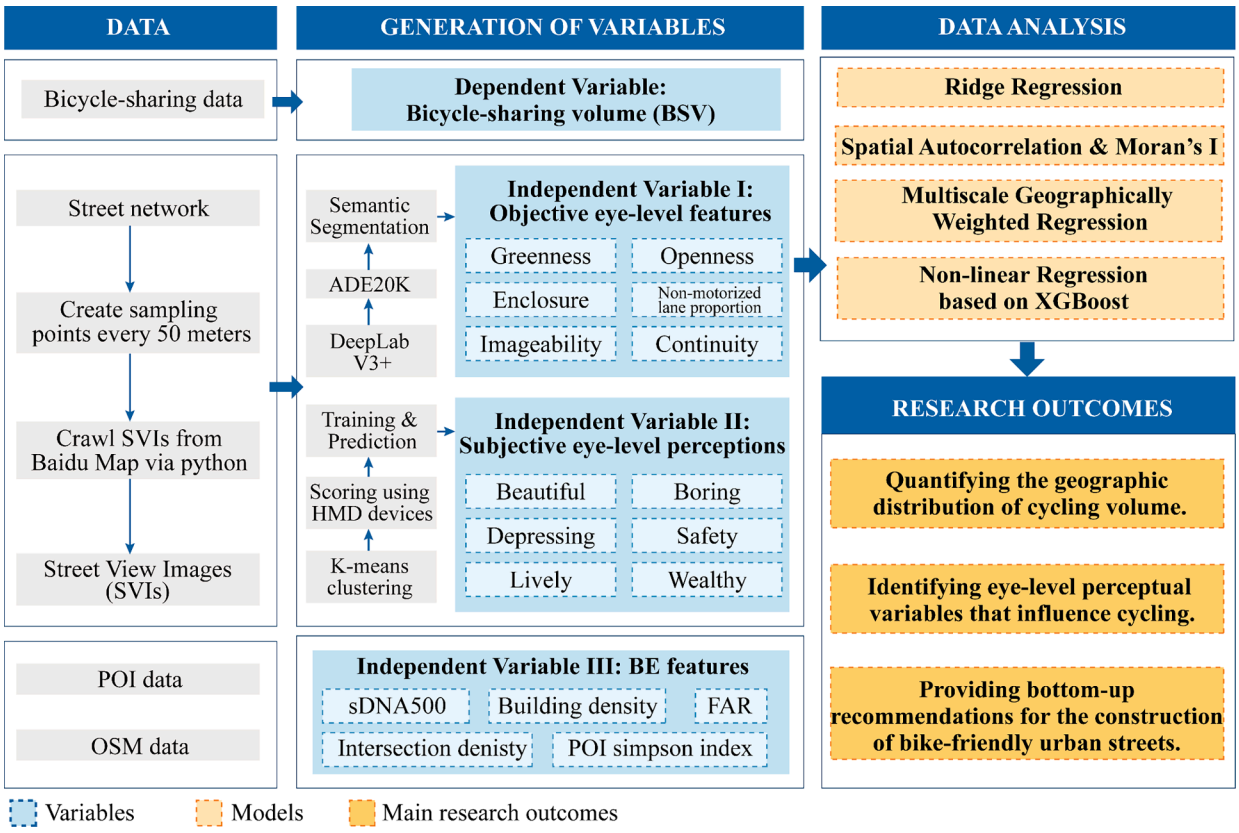

Fig. 1. Conceptual framework.

trajectories. Initially, an undirected graph was generated based on the road network downloaded from OSM. Subsequently, the starting and ending points of valid data were associated with the grid centroids. Rides that started and ended within the same grid were excluded, resulting in 46,191 origin-destination pairs. Furthermore, using the networkx library in Python (https://networkx.org/), the shortest road network path between each ride's start and end points was determined, generating 1,138,181 valid trajectories. BSV was calculated by dividing the total trajectory length within a plot by the street length inside that plot.

2.3.2. *Independent variable I: objectively measured eye-level streetscape perceptions*

Drawing upon previous studies (Ma et al., 2021; Rui, 2023b), six objective eye-level perceptual variables were selected: greenness, openness, enclosure, non-motorized lane proportion, imageability, and building continuity. Greenness refers to the presence of green landscape features such as grass, trees, vegetation, and green belts (Ma et al., 2021). Openness is the degree of visibility of the sky and determines the perceived brightness. Enclosure quantifies the level of human scale by measuring the proportion of vertical elements (Ewing & Handy, 2009). Non-motorized lane proportion is assessed by the ratio of the area of non-motorized lanes to the total area of streets, evaluating the outdoor environment's favorability towards non-motorized (active) travel (Rui, 2023b). The selection of this variable is based on two main reasons: Firstly, the issue of right-of-way allocation between sidewalks and bicycle lanes has not been resolved. Secondly, current pre-trained datasets for semantic segmentation classify road surfaces into motorized and non-motorized lanes, without further differentiation into pedestrian paths and cycling lanes. In addition, imageability refers to the ability of an urban landscape to evoke a clear and memorable image in the mind of an observer, driven by distinct shapes, colors, or arrangements (Lynch, 1964). Building continuity represents the unbroken and cohesive arrangement of structures in a BE, providing a consistent and harmonious streetscape or urban fabric (Wu et al., 2023). The calculation formulas and explanations for greenness, openness, enclosure, non-motorized lane proportion, imageability and building continuity is in Table 1.

2.3.3. *Independent variable II: subjectively measured eye-level streetscape perceptions*

We selected beautiful, boring, depressing, lively, wealthy, and safe as scoring indicators to reflect people's perceptions of the streetscape environment. Two thousand SVIs were chosen for subjective scoring, improving upon the method in prior research where the first 300 photos were directly selected (Wang et al., 2022). We employed the K-means clustering algorithm and random sampling to ensure that the sample better represented the overall characteristics of over 110,000 SVIs. To be more specific, we filtered out categories with an average proportion of less than 0.1% in the semantic segmentation results, yielding 19 categories for K-means clustering (Fig. 3.a.1). The silhouette score is a measure of how similar an object is to its own cluster (cohesion) compared to other clusters (separation). The higher the silhouette score, the more clearly defined the clusters are. In Fig. 3.a.2, it can be seen that the silhouette score peaks when k=5. Therefore, we set k at 5 to accommodate the diversity of street types.

We transformed SVIs into fisheye images suitable for virtual reality (VR) technology. In March 2023, we invited participants to rate the streetscape environment. A total of 100 participants aged between 21 and 45 were participated (58 males, 42 females). The average age of the participants was 27.5, with a standard deviation of 5.77. Before scoring, each participant was required to confirm they had normal vision and signed a consent form indicating their voluntary participation. Participants scored 6 subjective perception indicators using HDM-Devices based on a 7-point Likert scale (Fig. 3.b). In the Likert scale method, 1 represents the lowest, and 7 represents the highest. We weighted the

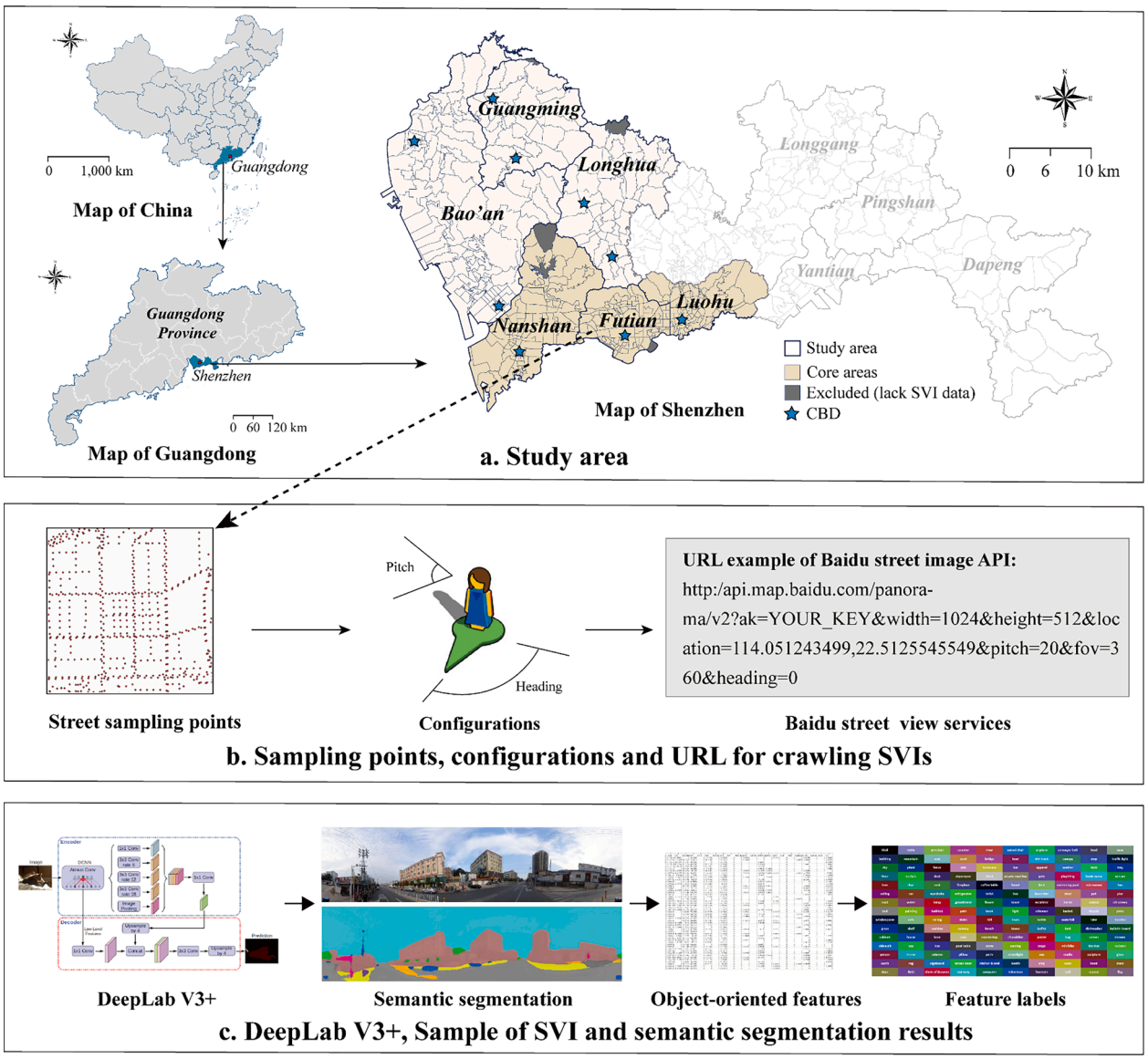

Fig. 2. Study area selection, and extraction and segmentation of SVIs in the study area. (a) Study area; (b) Sampling points, configurations and URL for crawling SVIs; and (c) DeepLabV3+, sample of SVI and semantic segmentation results.

scores from all participants to obtain the final score for each scored streetscape in the six subjective perception aspects. Lastly, using the same 19 semantic segmentation indicators as those used in K-means clustering, we built prediction models for the six indicators using XGBoost. Here, the proportions of 19 elements serve as independent variables to predict the subjective perception (dependent variable) of all street views in the study area, based on the average scores given by participants. The average R^2 for the 6 models is 0.24, and the average maximum error is 2.48, indicating a satisfactory prediction performance (Table 2).

2.3.4. *Independent variable III: built environment (BE) features*

We utilized sDNA (Hillier & Hanson, 1989), a spatial syntactic research tool to explore the street betweenness (De Nazelle et al., 2011). For residents engaged in leisure activities, a 500 m distance is walkable via a sidewalk or bike lane. Therefore, we adopted a radius of 500 meters to assess the potential for active travel in the selected area (Rui, 2023b; Thaler, 2020). Simultaneously, the Building Coverage Ratio (BCR) refers to the ratio of the ground area occupied by buildings to the total land area designated for building use. It reflects the degree of horizontal land occupation by buildings. The Floor Area Ratio (FAR) is the ratio of the total built-up area of buildings to the land area they occupy. This variable measures the vertical density of buildings. Street Intersection Density (SID) refers to the ratio of the number of street intersections in a specific area to the area size. It reflects the density and connectivity of the street network within the area and is associated with higher non-motorized lane proportion and better traffic flow. In addition, the Simpson index, known as Simpson's diversity index or Simpson's index of diversity, is a measure of diversity. Higher values of the index indicate greater diversity. In this study, the Simpson index was calculated for all POIs (SIP), commercial POIs (SICP), and public service facility POIs (SIPP). The formulas and explanations for the BE features are in Table 3.

2.4. *Model architecture*

2.4.1. *XGBoost and partial dependence plot (PDP)*

XGBoost is an ensemble machine learning algorithm based on decision trees, introduced by Chen and Guestrin (2016). It utilizes Classification and Regression Trees (CART) to classify and predict datasets. We opted for XGBoost based on its exceptional performance in handling the

Table 1
Formula and explanation of objective perceptions.

Formula	Explanation
$Greenness = \frac{\sum_{i=1}^{2} GP_i}{\sum_{i=1}^{2} P_i}$	GP_i denotes the proportion of green pixels, including plant, tree and grass; P_i is the total number of pixels in image i.
$Openness = SP_i$	SP_idenotes the proportion of sky pixels
$Enclosure = \frac{\sum_{i=1}^{2}(B_i + T_i + W_i + F_i)}{\sum_{i=2}^{2}(1 - SP_i)}$	B_i denotes the proportion of building pixels, T_i denotes the proportion of tree pixels, W_i denotes the proportion of wall pixels, F_i denotes the proportion of fence pixels.
$Non-motorized\ lane\ proportion = \frac{\sum_{i=1}^{2} SP1_i}{\sum_{i=1}^{2}(R_i + SP1_i)}$	R_i denotes the proportion of road pixels, and $SP1_i$ denotes the proportion of non-motorized lane pixels.
$Imageability = \frac{1}{2}\sum_{i=1}^{2}(S_i + S1_i + B_i + P2_i + B1_i)$	S_i denotes the proportion of signboard pixels, $S1_i$ denotes the proportion of sculpture pixels, $P2_i$ denotes the proportion of person pixels, $B1_i$ denotes the proportion of bench pixels.
Building continuity $= 1 - \lvert B_i - \overline{B_i}\rvert$	B_i denotes the proportion of building pixels, $\overline{B_i}$ denotes the average building ratio of individual streets.

data of this study. We compared the performance of decision tree, random forest, K-nearest neighbors (KNN), back propagation, support vector machines (SVMs), LightGBM, and XGBoost in training and testing our data, and found that XGBoost performed best (Table A 1). These models were constructed using a 5-fold cross-validation method from the Python package scikit-learn. The number of estimators was set to 1000, with maximum tree depths between 6 and 8, adjusted according to each model for optimal performance. The Partial Dependence Plots (PDPs) technique can provide insights into the impact of specific factors on the predicted outcome of a machine learning model (Greenwell, 2017).

2.4.2. Moran's I test and MGWR

The Global Moran's I index evaluates the overall spatial correlation pattern of attribute values of units in neighboring or adjacent regions across the entire study area (Moran, 1950). The formula of global Moran's I is as follows (Eq. (1)):

$$Global\ Moran's\ I = \frac{\sum_{i=1}^{n}\sum_{j=1}^{n} w_{ij}(x_i - x^-)(x_j - x^-)}{S^2 \sum_{i=1}^{n}\sum_{j=1}^{n} w_{ij}} \quad (1)$$

Where n is the number of UVs, x_i and x_j respectively represent the urban ATI of region i and j, and w_{ij} is the spatial weight matrix.

The Geographically Weighted Regression (GWR) was proposed by Brunsdon et al. (1996), based on constructing a regression model with a spatial weight matrix. It is widely used for analyzing spatial influencing factors. MGWR was introduced by Fotheringham et al. (2017). MGWR enhances the traditional GWR model by assigning a unique bandwidth to each variable. The formula is as follows (Eq. (2)):

$$Yi_i = \sum_{j=1}^{k} \beta_{bij}(u_1, vi_i)x_{ij} + \varepsilon_i \quad (2)$$

β_{bij} represents the regression coefficient of the local variable, *bij* represents the bandwidth used by the regression coefficient of the variable j, and (u_i, vi_i) represents the spatial coordinates of the sample point i, x_{ij} is the observed value of the variable j at the sample point i, and ε_i is the random disturbance term.

3. Results

In the Results section, we present the geographical distribution of BSV. The distribution of independent variables is shown in Fig. A 1 and Fig. A 2. The Pearson correlation of all variables in shown in Fig. A 3. Subsequently, we display the results of nonlinear-regression and spatial regression models. We conducted a joint analysis of statistical and geographical regression for the independent variables for further explanation.

3.1. Descriptive analysis of bicycle-sharing volume (BSV)

Fig. 4.a displays the geographical distribution of BSV. We observed that the high and low values of BSV within the study area are dispersed. All data has been normalized. Elevated levels of BSV are primarily located in the Futian, the southern part of Longhua, and the western part of Luohu District, with the clustering effect in Longhua District being especially pronounced. In contrast, the Nanshan District does not exhibit high-value clustering. Meanwhile, lower values are found in the suburban areas, particularly in the Guangming, Bao'an, and the northern part of Longhua District, where there is a continuous low value. Notably, the geographical disparity in BSV in Longhua District is the most significant, with low values in the north and high-value in the south, indicating an uneven distribution of bicycle-sharing in this area.

Fig. 4.b illustrates the BSV during different times of the day. Throughout the day, the proportions of bicycle-sharing durations of 1-5min, 5-10min, 10-20min, 20-30min, and over 30min are 25.15%, 37.87%, 26.19%, 6.38%, and 4.41%, respectively. Only 10% of rides last more than 20 minutes. We observed that shared bicycle trips are predominantly short distances of less than 5km. In addition, the BSV exhibit distinct morning and evening peak periods, with the morning peak clustered around 7-9 a.m. and the evening peak appearing between 17-19 p.m.

In addition, the statistical description and geographic distribution of the independent variables are shown in Table A 2 and Appendix A. Descriptive Analysis of dependent variables, respectively.

3.2. The performance of model results

The R^2 value for XGBoost reaches 0.203. The importance ranking of variables shows that streetscape perceptions and the BE both have an impact on BSV (Fig. 5). Among them, sDNA500 is the most important for BSV. In terms of the objective eye-level perceptions, openness, greenness, and building continuity rank in the top three. In terms of subjective streetscape perceptions, beautiful, imageability, and lively occupy the top tier rankings. Eye-level streetscape perceptions play a significant complementary role for the BE, where the ranking of objective perceptions is ahead of subjective perceptions. This finding underscores the significance of our bottom-up approach, emphasizing the human-eye perspective in influencing BSV.

We posit that streets serve as the primary conduits for bicycle-sharing travel. The street accessibility significantly influences residents' choice to opt for bicycle-sharing behavior and route selection. From an eye-level perspective, the openness of streets suggests the sight extension or be covered by shadow of trees, fostering positive environmental psychological perceptions. Streets characterized by high openness and green visibility offer cyclists a comfortable riding experience (Nawrath et al., 2019; Rui, 2023b). Moreover, a higher SIPP indicates a greater availability of nearby public services and encourages residents to choose active transit options, such as shared bicycles. Similarly, a higher FAR suggests greater land-use efficiency in the area.

The Global Moran's I Index for BSV is 0.516, with a z-value of 18.915 and a p-value of 0.000, meeting the requirements for geospatial regression, as shown in Table A 3. The R^2 for MGWR stands at 0.576 with an adjusted R^2 of 0.488, representing a significant improvement over XGBoost. This suggests that there might be a more pronounced geographical relationship between BSV and streetscape perception and the BE.

3.3. Joint interpretation of variables using multiple regression models

In our study, seven variables from MGWR were identified for their

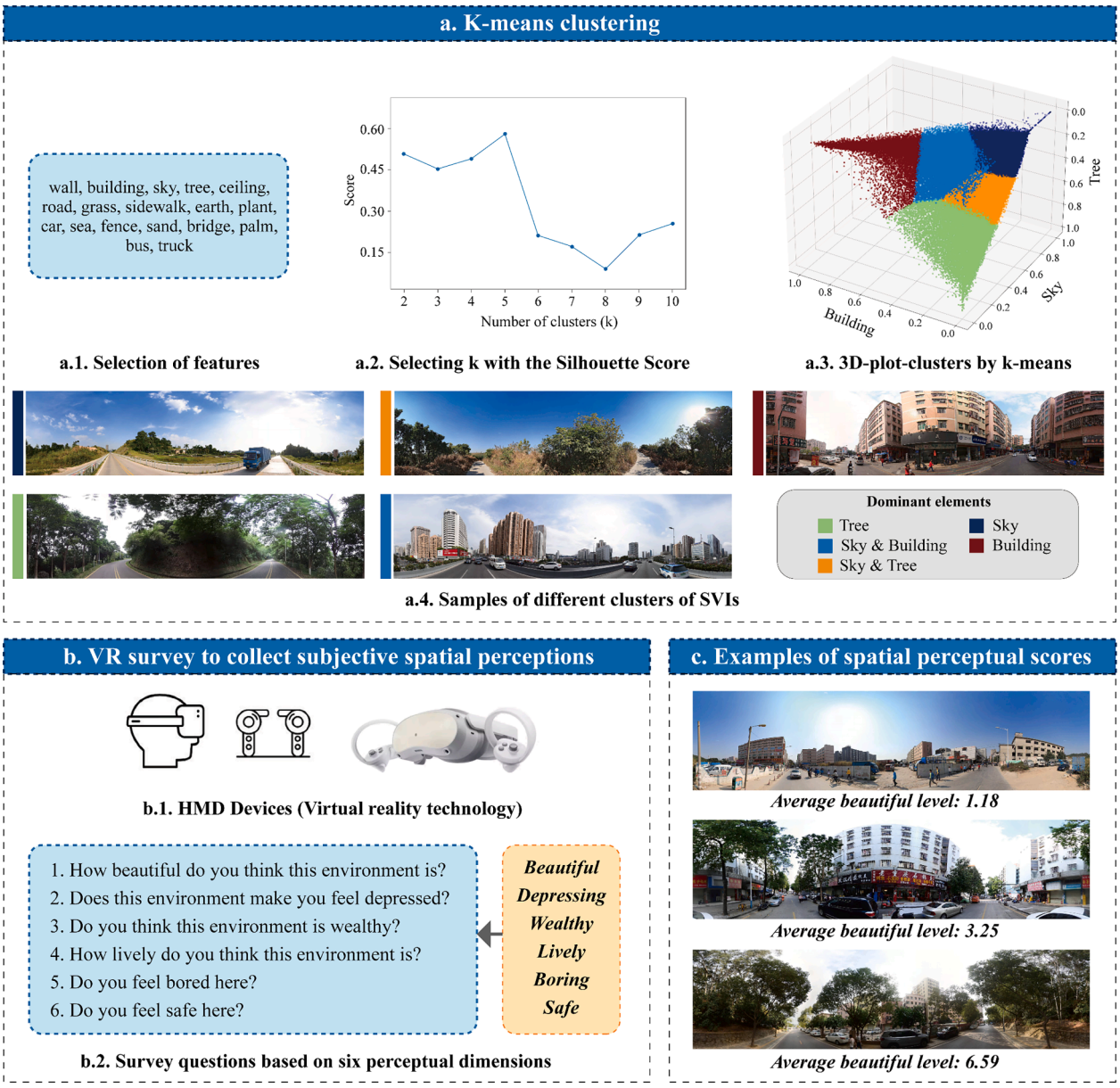

Fig. 3. (a) K-means clustering; (b) VR survey to collect subjective spatial perceptions; and (3) examples of spatial perceptual scores.

Table 2
Model performance for XGBoost in predicting subjective perceptions.

	Beautiful	Boring	Depressing	Safe	Lively	Wealthy	Mean
Mean squared error	0.62	0.64	0.58	0.73	0.64	0.63	0.64
Mean absolute error	0.63	0.63	0.61	0.67	0.64	0.64	0.64
R-Squared value	0.32	0.16	0.21	0.24	0.20	0.28	0.24
Max error	2.63	2.47	2.20	2.79	2.49	2.31	2.48
Explained variance score	0.32	0.16	0.21	0.24	0.20	0.29	0.24

notable spatial variations and were selected for further examination. By integrating multi-models (linear, non-linear, and geographical regression models), we aim to unveil the synergistic and conflicts between perceptions, BE variables and BSV.

3.3.1. Objective eye-level perceptions (greenness and building continuity)

PDP results indicate that within a coefficient range of 0.2-0.3 (after standardization), an increase in the greenness promotes BSV (Fig. 6.a.2). However, when the coefficient exceeds 0.3, BSV significantly decreases, showing a weak positive relationship. The results of MGWR indicate that these weak positive relationships are mainly found in the eastern part of Luohu and the central area of Longhua, while strong positive correlations exist in the Nanshan district and the western part of the Bao'an district in Shenzhen (Fig. 6.a.1).

Although Nanshan, Futian, and Luohu District are central urban areas, the BSV in Nanshan and eastern parts of Luohu is significantly lower than that in the southern part of Longhua. The greenness index in the central part of Nanshan and the eastern part of Luohu consistently

Table 3
Formulars and explanations of built environment feature.

BE features	Formulas	Explanations
sDNA500	$\boldsymbol{Betweenness}_{(x)} = \sum_{y \in N z \in R_y} W_{(y)} W_{(z)} P_{(z)} OD_{(y,z,x)}$ $\boldsymbol{OD}_{(y,z,x)} =$ $1,\ if\ x\ is\ on\ the\ first\ geodesic\ found\ from\ y\ to\ z$ $1/2,\ if x = y \neq z$ $\{\ 1/2,\ if\ x = z \neq y$ $1/3,\ if\ x = y = z$ $0,\ otherwise$	In the formula, W(y) is weight of a polyline y and W(z) is weight of a polyline z; P(z) is the proportion of any polyline z within the radius. OD represents the origin destination. The geodesic endpoints are y and z, not x where the betweenness is being measured. The contribution of 1/2 to OD (y,z,x) reflects the end links of geodesics, which are traversed half as often on average, as journeys begin and end in the link center on average. The contributions of 1/3 represent the origin of self-betweenness.
Building density	$\text{Building Density} = \frac{T_B}{T_A}$	T_B denotes the total built-up area, T_A denotes the total area of the study unit.
Floor Area Ratio (FAR)	$\text{FAR} = \frac{T_F}{T_A}$	T_F denotes the total floor area of the building, T_A denotes the total area of the study unit.
Street intersection density (SID)	$\text{SID} = T_I$	T_I is the count of street intersections identified within the study unit.
Simpson index of POIs	$Simpson\ index = 1 - \sum_{i=1}^{n} (N_i/\mathrm{N})^2$	N_i represents the number of the ith type of POI within the study unit. N represents the total number of POIs. n represents the total number of POI types.

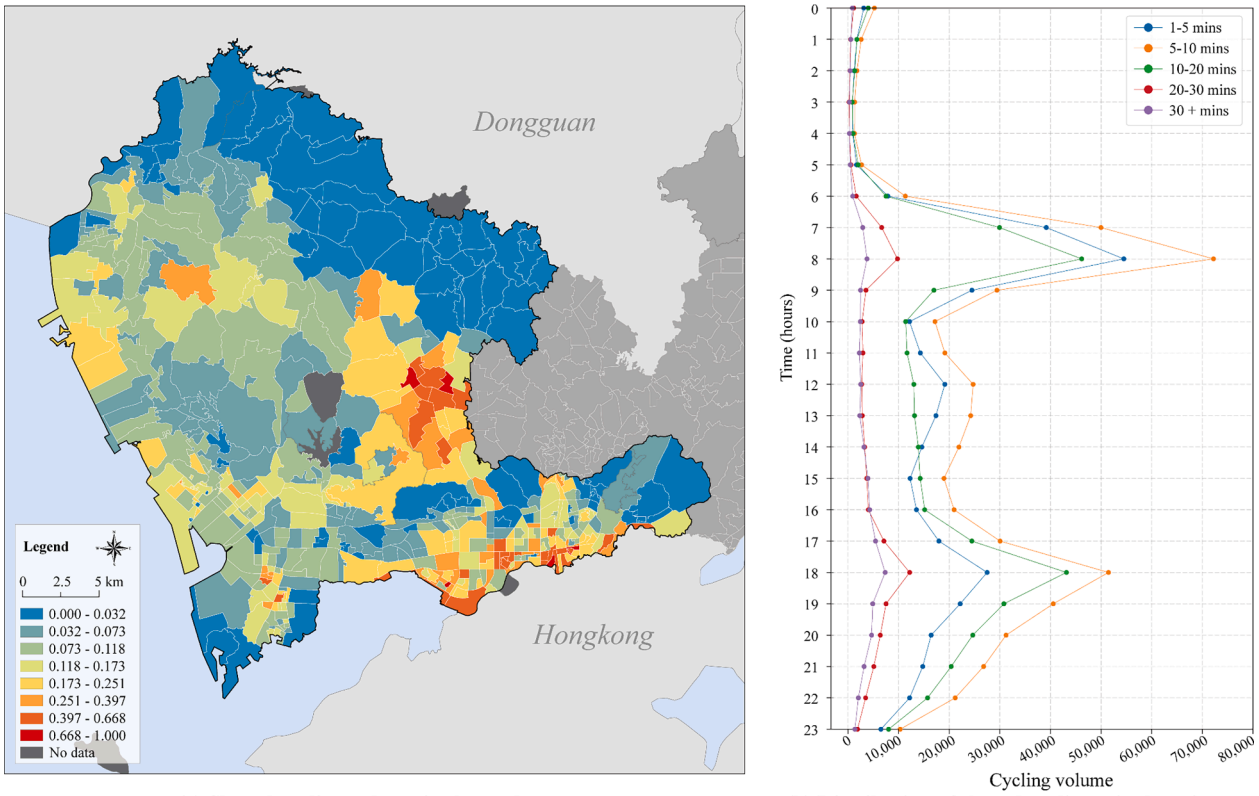

(a) Shared cycling volume in the study area. **(b) Distribution of shared cycling trip durations.**

Fig. 4. (a) Bicycle-sharing volume in the study area; (b) distribution of bicycle-sharing trip durations.

higher than Longhua. This discrepancy is one of the reasons for the negative correlation observed in MGWR results. The MGWR analysis illuminates a positive correlation between the FAR and BSV, with salient manifestations in the Futian and Luohu Districts (Fig. 6.b.1). We postulate that urban cores with high FAR, influenced by prevailing land valuations and functional imperatives, inevitably require a denser BE. Hence, precincts within Futian and Luohu exhibiting pronounced BSV could potentially experience a paucity of expansive green spaces, such as trees and lawns. In Futian and Luohu, which exhibit elevated BSV, there might be a notable deficit in trees and lawns. This scarcity subsequently establishes a negative correlation between greenness and BSV within central urban areas.

One-way PDP (Fig. 6.b.2) indicates that BSV is at its lowest when the building continuity coefficient ranges between 0.7 and 0.8. From the MGWR results, building continuity displays a positive correlation with BSV in both Futian and Luohu Districts, while in other districts, the correlation is negative. Specifically, the positive correlation is most pronounced in the southern part of Futian and the eastern part of Luohu. Conversely, the strongest negative correlation is observed in the southern areas of Nanshan and Longhua Districts. As central urban areas, both Futian and Luohu are characterized by higher land values and dense construction. Consequently, there's enhanced building continuity in these districts, which correlates positively with BSV. Continual building façades often evoke a sense of monotony. From the two-way PDP (Fig. 6.b.3) concerning boring and building continuity suggest that areas with the least building continuity often align with reduced boring index and the highest BSV. Intriguingly, the impact of building continuity is less pronounced than the boring index. Potential explanation posits that such perceptions of boring may be modulated by other environmental features. Hence, we advocate for interventions that

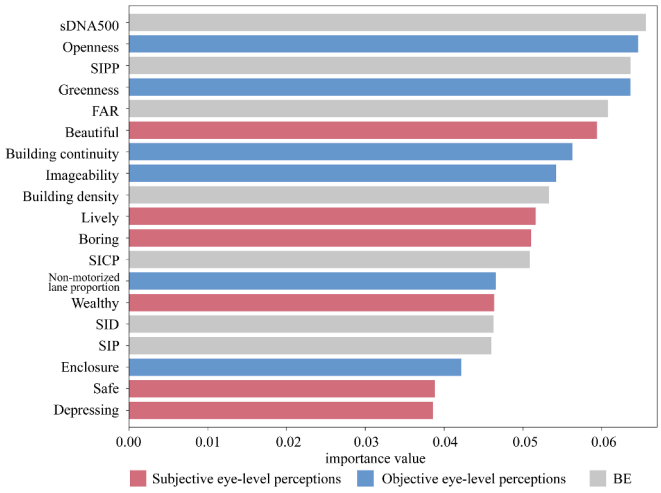

Fig. 5. Feature importance of eye-level perceptions and BE.

disrupt the monotony of continuous street façades—such as diversifying building heights and integrating architectural nuances—to potentially enhance the appeal of bicycle-sharing.

3.3.2. *Subjective eye-level perceptions (beautiful and wealthy)*

The PDP (Fig. 6.c.2) reveals a rising trend in BSV corresponding to increases in the "beautiful" coefficient, though this trend appears to stabilize within the 0.5-0.7 interval. MGWR findings suggest a gradual north-to-south increase in the positive influence of the beautiful index on BSV (Fig. 6.c.1). Streets perceived as most beautiful index are predominantly situated within the Nanshan and Futian districts. Joint with the two-way PDP for sDNA500 (Fig. 6.c.3), it becomes evident that moderate street connectivity (within a standardized coefficient range of 0.2-0.25) and a moderate beautiful index (within a standardized coefficient range of 0.4-0.55) markedly bolster BSV. As outlined in the *Shenzhen Bicycle Transportation Development Plan (2021-2025)*, the prevailing spatial quality of cycling paths in Shenzhen is suboptimal, plagued by issues such as overly narrow pathways, obstructed sightlines, and chaotic road circulation. Therefore, in the discussion section, we will identify these streets, aiming to bolster bicycle-sharing propensity through tailored street design recommendations.

Geospatial analysis reveals distinct clusters of high "Wealthy" index within the southern sector of Longhua District, the central-eastern area of Futian District, and throughout Nanshan District (Fig. A 1). MGWR results demonstrate that the BSV in the southern part of Longhua and the central-eastern part of Futian has a strong correlation with the "Wealthy" index (Fig. 6.d.1). In contrast, despite its elevated "Wealthy" index, Nanshan District presents a negative correlation. As a central urban area, the overall planning of Nanshan District prioritizes motor vehicle traffic to avoid congestion (*Nanshan District, Shenzhen Urban Land Use and Spatial Planning 2021-2035*) (Shenzhen Municipal Planning and Natural Resources Bureau, 2023). Furthermore, we identified two areas in the southwestern part of Nanshan District with high BSV, namely the Nanyuan Community and the Nanyou A Zone. These areas are designated as urban village residential lands, as lower-income groups tend to favor more affordable public transportation options. According to the *Main Conclusions of the Seventh Resident Travel Survey in Shenzhen* (Shenzhen City Planning and Land Development Research Center, 2021), the educational level of residents in Futian and Nanshan is significantly higher than other districts. Higher education levels leading to increased income have resulted in a greater proportion of private car usage and a reduction in bicycle travel (Niu & Chai, 2022; Shaaban, 2020). One-way PDP shows that BSV increases with the enhancement of the perception of wealthy (Fig. 6.d.2). Overall, areas with elevated levels of perceived wealth record a higher prevalence of bicycle-sharing.

3.3.3. *BE factors (building density, SICP, and SIPP)*

Building density demonstrates a weak negative correlation with BSV in MGWR (Fig. 7.a.1), presenting a decreasing trend from northwest to southeast, with the lowest values appearing in Futian and Luohu districts. The PDP indicates that BSV decreases with an increase in building density and a reduction in the FAR. The geographical distribution of building density (Fig. A 2.b) can elucidate the negative correlation with BSV. From the distribution of urban villages in Shenzhen (see Supplementary material), it becomes evident that regions in Bao'an, Guangming, and Longhua District with high building density (Fig. A 2) predominantly correspond to the industrial urban villages (Rui & Li, 2023). Given their location on the suburbs, the availability of shared bicycle pick-up and drop-off points is limited. However, this does not imply a diminished demand for shared bicycle rides for workers in these areas. It is encouraged to increase the number of bicycles pick-up/drop-off points, thus promoting low-carbon transportation among urban village residents (Rui, 2023a).

One-way PDP indicates that the coefficients of simpson index of commercial POIs (SICP) and simpson index of public service POIs (SIPP), within the range of 0.8 to 0.95, have minimal impact on BSV (Fig. 7.b.2 and c.2). However, as the coefficients extend beyond 0.95, they significantly enhance BSV. Two-way PDP reveals a clear synergistic effect of the richness of these two POIs on the increase of BSV (Fig. 7.b.3). MGWR results demonstrate that simpson index of commercial POIs exhibits the strongest positive correlation with BSV in the western area of Longhua, while simpson index of public service POIs does not show significant numerical differentiation. The influence of simpson index of commercial POIs on BSV may be closely tied to data sourced from weekdays. Commercial functions accommodate a large number of employment, and the working population is likely to cycle on shared bicycles following a metro commute (Parkin et al., 2008). In contrast, travels aligned with public service objectives, encompassing medical appointments, schooling, and official business, primarily involve minors, students, patients, and administrative personnel. Punctuality and transportation reliability are crucial considerations for these populations (Haustein et al., 2018; Lin et al., 2020). Given that shared bicycles cannot guarantee consistent timing and costs compared to other commuting modes like metros or buses, they are often superseded by alternative transportation methods (Meng et al., 2016).

4. Discussion

4.1. *Synergistic advantages of multiple regression models in explaining BSV*

We utilized multiple models to co-interpret the relationship between BSV, eye-level streetscape perceptions and BE. According to further analysis using XGBoost, we found that there might be two reasons behind: Firstly, people choose shared bicycles for commuting purposes on weekdays, preferring shorter routes rather than streets with high greenery rates. Secondly, areas with high supply and demand for shared bicycles tend to be high-density urban CBDs, hence offering limited space for planting streetscape vegetation.

We explored the marginal effects of each feature on BSV and the joint effects of two variables on the outcome using PDPs. Due to the distribution of training data and algorithm precision, the PDPs exhibited noticeable fluctuations. For instance, the one-way PDP for FAR displayed a stair-step upward trend. To address this, we fitted spline curves to reflect the overall trend, effectively enhancing the interpretability of the XGBoost model and PDP results. In addition, the fitting performance of MGWR showed significant improvements compared to both linear and nonlinear regressions. This indicates a more pronounced geographical relationship between BSV, eye-level streetscape perceptions and BE.

The combination of XGBoost and PDPs revealed the nonlinear relationship between variables with BSV. Likewise, the feature importance

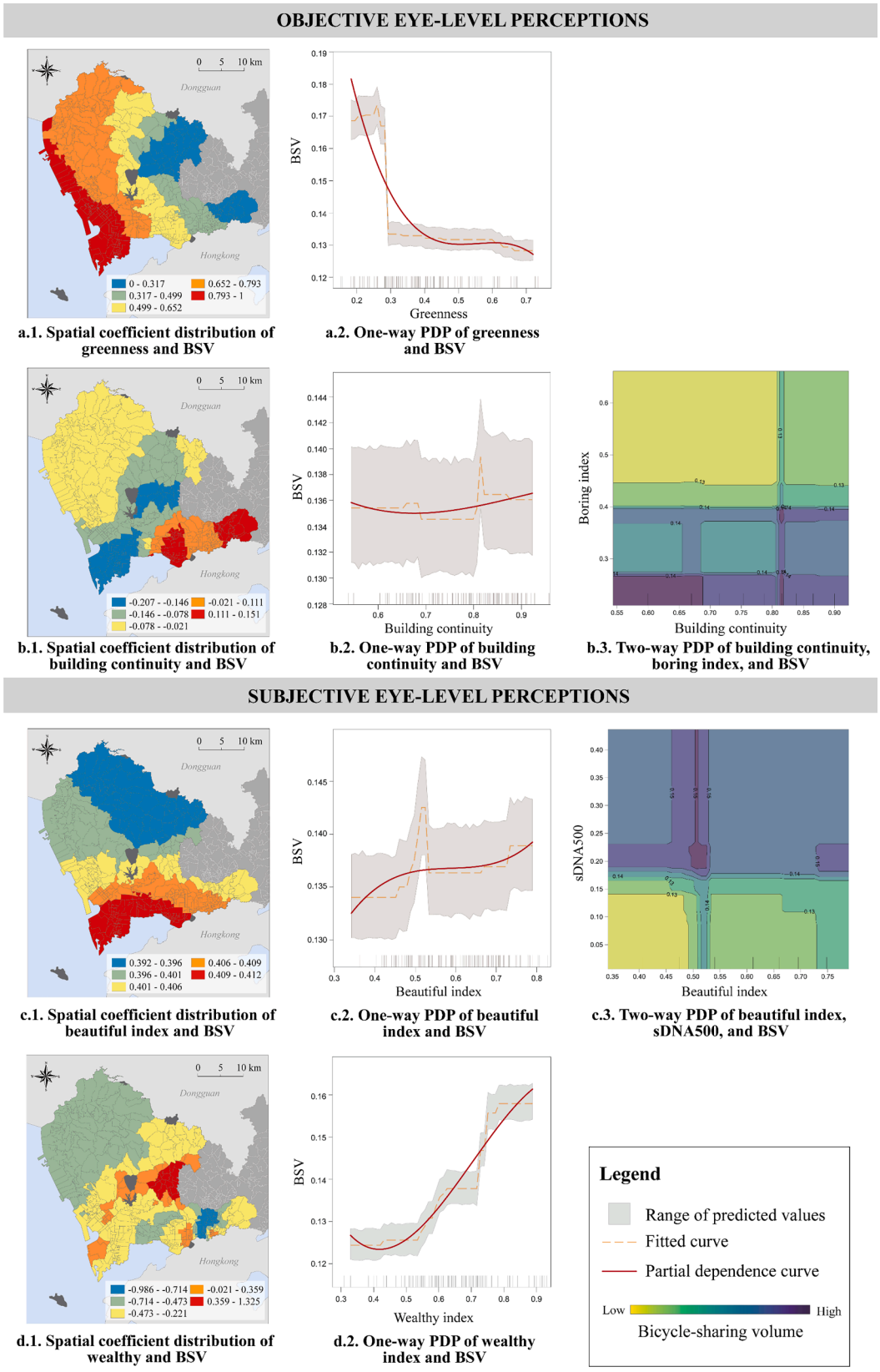

Fig. 6. Joint analysis of objective and subjective eye-level perceptions on bicycle-sharing volume.

ranking and two-way PDPs further assisted us in comparing the significance of variables. In addition, the MGWR results elucidated the spatial heterogeneities in BSV, allowing us to pinpoint region-specific challenges and propose targeted measures.

4.2. Shaping bicycle-sharing-friendly streets through micro perspectives

We observed substantial spatial variations between the streetscape quality and BSV in Shenzhen. Consequently, we utilized quantified eye-

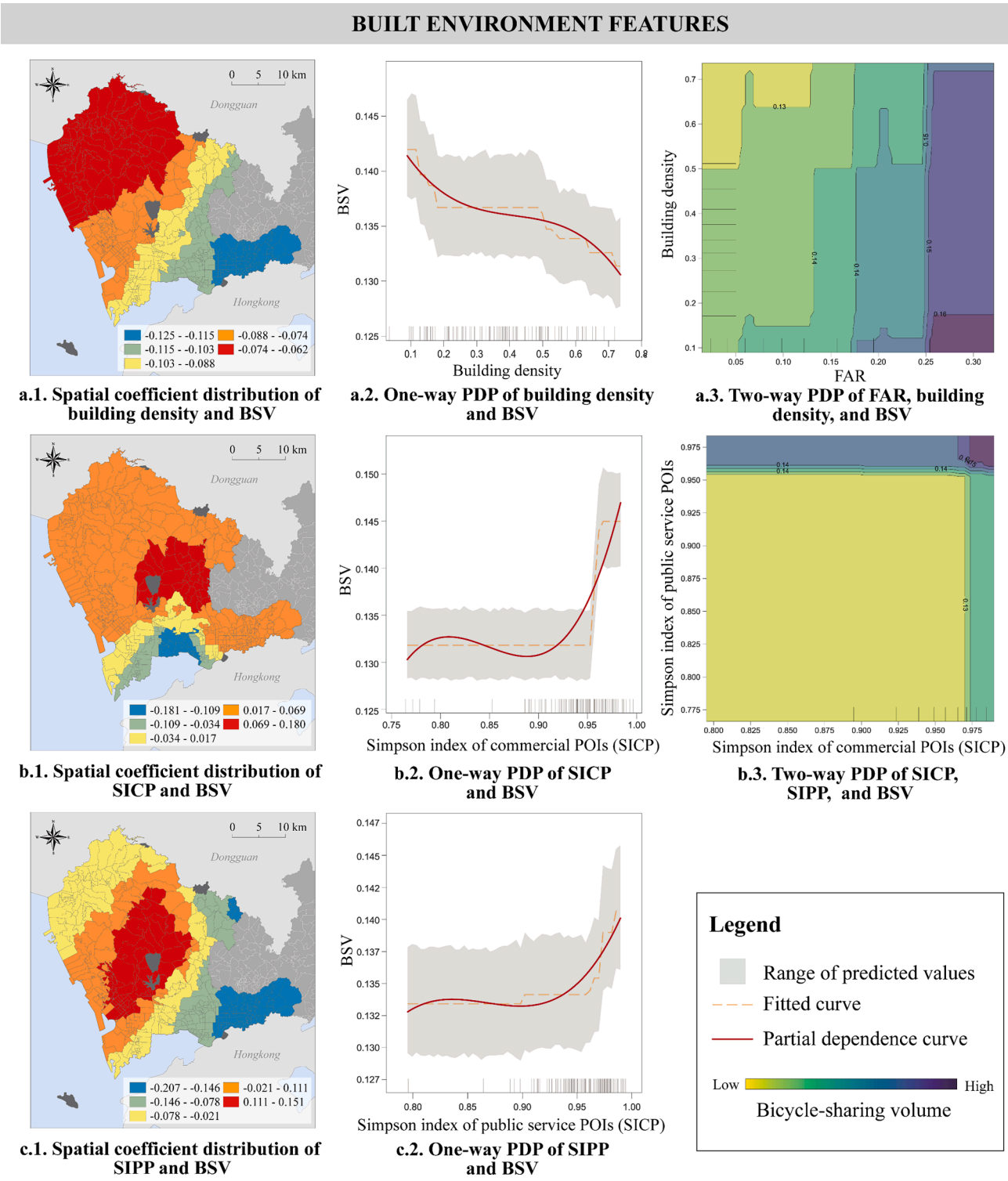

Fig. 7. Joint analysis of the BE on bicycle-sharing volume.

level perceptions to compute an overall score for street perceptual quality (SPQ) and matched it with BSV. This approach allowed for identification of cycle-friendly urban streets and those that require spatial improvement, further delineating a prioritization framework for these modifications. Within the six subjective perceptions, "beautiful," "safe," "lively," and "wealthy" were given positive values; whereas "boring" and "depressing" were assigned negative values. Each category employed coefficients from the importance of XGBoost. The calculation of SPQ score is shown below (Eq. (3)):

$$\begin{aligned}\textbf{\textit{Street perceptual quality}}\ (\textbf{\textit{SPQ}}) = {} & 0.0594 \times \overline{\textbf{\textit{Beautiful}}} + 0.0388 \\ & \times \overline{\textbf{\textit{Safe}}} - 0.03859 \times \overline{\textbf{\textit{Depression}}} \\ & - 0.0510 \times \overline{\textbf{\textit{Boring}}} + 0.0516 \\ & \times \overline{\textbf{\textit{Lively}}} + 0.0463 \times \overline{\textbf{\textit{Wealthy}}}\end{aligned} \tag{3}$$

According to Fig. 8.a, the high values of SPQ decrease from the

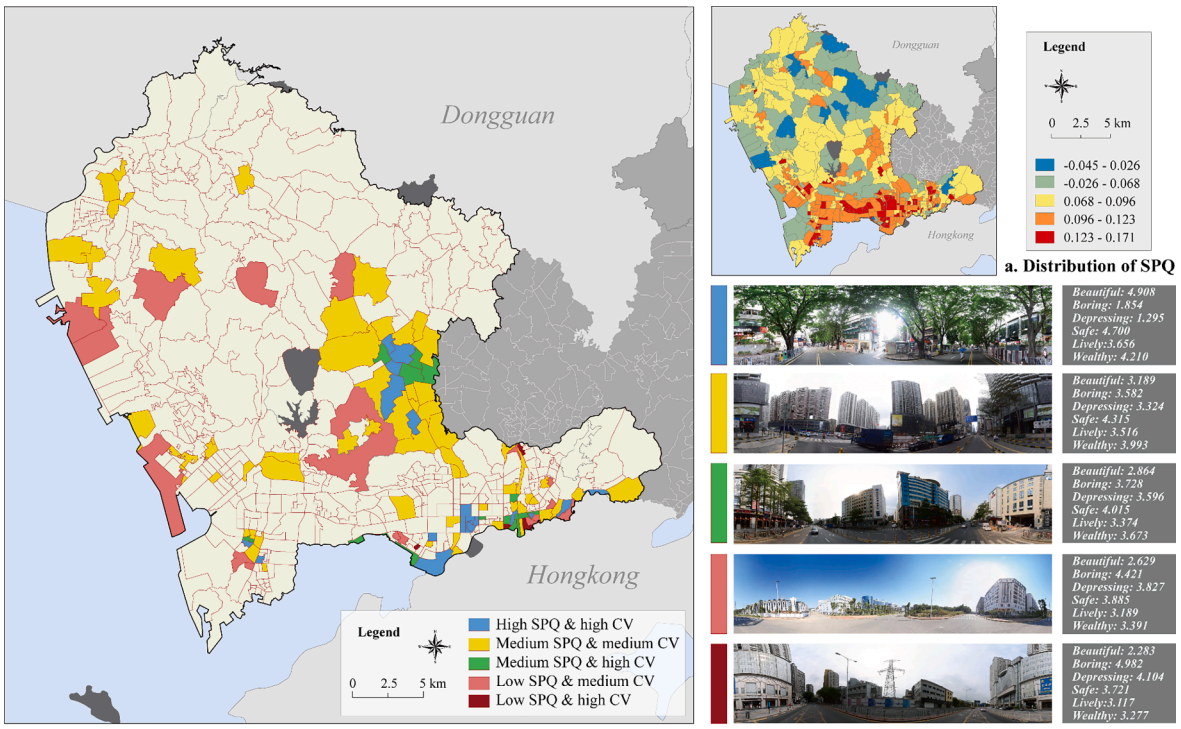

Fig. 8. (a) Distribution of SPQ; (b) classification of eye-level perceptual scores and bicycle-sharing volume; and (c) random sampling of SVIs based on the classification.

central urban area to the suburbs, exhibiting a positive correlation with the maturity of the urban development. The high level of development and dense BE of CBDs in different districts amplify the perceptions of "wealthy", "lively", and "safety". Within our study area, the highest SPQ is concentrated in the eastern part of Nanshan, central Futian, and the western part of Luohu District. Conversely, the most significant concentration of BSV is found in the central-southern part of Longhua, along with the western regions of Futian and Luohu Districts.

Notably, BSV also geographically diverges from SPQ. The central-southern part of Longhua District exhibits high BSV, but only moderate SPQ, while Nanshan boasts commendable SPQ yet exhibits lower BSV. We postulate that such discrepancies arise due to the following factors: First, polycentric urban structure in Shenzhen offers proximate employment opportunities, diminishing the necessity to commute to the core area. Second, owing to developed metro system, residents often opt for the efficiency and temporal reliability of the metro over shared bicycles for medium to long-distance commutes. Third, the *Shenzhen's 13th Five-Year' Urban Renewal Plan* (Shenzhen Municipal Bureau of Planning and Natural Resources, 2019) indicates large-scale urban village demolition and comprehensive renovations in central areas. Newly constructed commercial housing in these central zones attracts higher income groups, accelerating the process of gentrification (Rui, 2023a). These affluent demographics tend to prefer car travel, thus reducing the use of shared bicycles.

We employed a classification method to further analyze the SPQ and BSV, aiming to identify streets where cycling-oriented renovation should be prioritized. Using the natural breaks method, we categorized both SPQ and BSV into three clusters: high, medium, and low. In Fig. 8.b, blue zones represent high SEQ coupled with high BSV; yellow regions correspond to medium SEQ and medium BSV; green areas depict a medium SEQ with high BSV; light red areas signify a low SEQ with medium BSV; and dark red zones indicate a low SEQ with high BSV.

Colors designated as blue (Level I), yellow (Level II), light red (Level III), green (Level III), and deep red (Level IV) are recommended in a hierarchy for urban renewal prioritization. As increasing levels signify escalated renovation urgency, serving as a guidepost for redevelopment initiatives. From Fig. 8.c, we discern that streets exhibiting both high SPQ and BSV are often characterized by a harmonious enclosure formed by tree and buildings, providing cyclists an enveloped sense of security. Physical segregations at the curbside serve to mitigate vehicular collision risks, clearly demarcating right-of-way. Certain vehicular lanes are further delineated with dedicated bus-only lanes, enhancing public transportation efficacy and forging a complementary dynamic with shared bicycle commuting. Moreover, the diversified ground-floor facades enrich the elements and color palette of the street, enhancing the street's imageability and creating a vibrant ambiance.

Level I: These areas also exhibit good enclosure. We observed distinct zebra crossings at street intersections to ensure the safety of slow-moving traffic. Additionally, street-side signage and physical barriers within the streets provide safety measures without obstructing sightlines.

Level II: In this area, we discerned street-side physical barriers, dedicated bicycle docking stations, well-organized shared bicycles, and a modest presence of sidewalk shops, corroborating the suitability for high BSV. Regarding streetscape quality, there's a noticeable decrease in enclosure compared to level I. Considering warm climate in Shenzhen, the planting of avenue trees remains essential. Furthermore, the dated architectural facades and predominance of mid to low-rise structures might amplify a sense of boring, potentially diminishing the aesthetic appeal.

Level III: The streetscape here is noticeably more monotonous and open. Cyclists are directly exposed to the thoroughfare rather than being sheltered. Hence, there's a need to cultivate more enclosing streetscape greenery. In our observations, the roads in the light-red zones lacked physical separations or dedicated bicycle lanes, presenting merely distinct pedestrian lane and vehicular lanes. This constrains the space available for bicycle-sharing and poses safety risks, particularly the potential for collisions with vehicles or pedestrians. Moreover, the streets of lower spatial quality lack vivid

facades and show an absence of commercial signage, which is related to the surrounding monolithic land use patterns.

Level IV: These areas exhibit the highest level of BSV, yet have the lowest SPQ score, making it the top priority for redevelopment. Our observation reveals an absence of street trees in these zones, failing to provide essential shading for cyclists and undermining the overall streetscape aesthetic value. Additionally, the broad streets are merely divided into motorized and non-motorized lanes. Hence, planners could consider designing bicycle-only lanes. Furthermore, the ground floor of street-front facades could be enriched with shops and shared bicycle facilities. A potentially controversial aspect might be the presence of street graffiti, as its symbolism varies across different countries and cultures. In the context of Shenzhen, street graffiti might diminish spatial aesthetic, evoking an impression of urban deterioration. Lastly, there are also recommendations to incorporate additional small-scale street infrastructure, such as cycling and road signs, streetlights, to enhance the safety and vibrancy of the bicycle-sharing environment.

4.3. Implications for long-term cycling-oriented policies

Micro-scale streetscape modifications represent a short-term, efficient measure to promote cyclist-friendly street designs and SMS. In the long run, it's also imperative to alter residents' travel behaviors and mode choices. Conclusions drawn from BE factors underscore the significance of commercial service density. The relationship between metro and shared bicycles, however, is relatively dynamic. This is because residents weigh the convenience, punctuality, and efficiency of both modes based on their travel purpose, such as medical appointments, employment, education, or recreation. Generally, residents are more inclined to opt for metro over shared bicycles for long distance travel. Yet, in districts with a high metro density like Futian and Luohu, shared bicycles exhibit a synergistic rather than a substitutive effect with the metro system (Fan & Zheng, 2020).

There exists a virtuous cyclical relationship between augmenting BSV and crafting a bicycle-friendly streetscape. During urban regeneration, it becomes pertinent to consider expanding or adding bicycle lanes in central urban areas to refine the non-motorized transportation system. In areas where land use is extremely constrained, catering to residents' transit needs can be achieved by enhancing the carrying efficiency of rail transportation. The symbiotic relationship between the metro system's efficacy in facilitating long-distance commutes and shared bicycles' role in bridging the "last mile" gap has invigorated BSV within these areas. Consequently, while promoting for bicycle-friendly policies, the advancement of comprehensive urban transit networks assumes a constructive, complementary role.

Urban transportation management policies stand as pivotal instruments to regulate motorization and congestion. The primary objective is to harmonize the relationship between supply and demand. On the demand side, residents' demands for shared bicycles exhibit uncertainty and elasticity. Therefore, on the supply side, beyond considering the construction of bicycle-sharing infrastructure, the government must also collaborate with shared bicycle operators to make joint decisions regarding the optimal distribution and allocation of shared bicycles, grounded in current bicycle-sharing patterns. Bicycle-sharing demands in Shenzhen vary distinctly across regions due to differences in socio-economic development, land-use, and transportation infrastructure. Hence, it becomes imperative to delineate region-specific frameworks for scheduling and governance. For instance, in urban central areas, upon refining bicycle-sharing infrastructure, road tolls and public transit subsidies can be leveraged to ensure bicycle-sharing assumes a role in handling short-to-medium distance trips and transit connections. In core areas such as Nanshan District, and the suburban industrial zones, the deployment of shared bicycles might be limited. Future research could identify potential supply gaps in shared bicycle provisioning within these areas. An augmentation in the supply of shared bicycles could serve as a catalyst in fostering active commuting.

5. Conclusion

Our study aims to elucidate the relationship between BSV, the eye-level streetscape perceptions and BE. We sourced millions of pieces of bicycle-sharing data from the Shenzhen Open Data Platform and quantified the BSV within the study area. Methodologically, we employed deep learning algorithms in conjunction with collected scoring questionaries to derive objective and subjective streetscape perceptions from a cyclist's viewpoint using SVIs. Additionally, key BE variables were included as complementary factors. Drawing upon existing research, we optimized the method for calculating the objective attribute of building continuity by taking geographical relationships into account. We further refined predictive models for calculating subjective streetscape perceptions through K-means clustering algorithms and HMD technology. Notably, we employed a synergistic approach, amalgamating XGBoost and MGWR models, to explore the numerical and geographic relationship.

Economic growth and urbanization have propelled motorized transportation into a dominant role, leading to urban traffic congestion and air pollution. Bicycle-sharing as an active mode of transportation aligns with the SDGs. Therefore, fostering residents' bicycle-sharing behaviors has become an integral task in current agendas. Shared bicycle paradigm in China offers cities a mechanism to enhance the proportion of bicycle commuting. Our investigation underscores that shared bicycle commuting in Shenzhen has carved out a pivotal role within the city's transportation framework. Our findings substantiate that improving the quality of the streetscape is one of the efficient strategies to bolster urban health and livability. By delving into the relationship between BSV and streetscape perceptual quality, we discern the imperative for tailored interventions across varied urban districts to refine streetscape conditions, thereby catalyzing BSV and promote SMS.

This study has two limitations. On one hand, the SVIs were acquired on February 15, 2023. Although the acquisition dates of SVI data and the bicycle-sharing data were within the same month, the shooting dates of the SVIs were not during the same timeframe. Differences in the SVI capture times could result in biases in the streetscape perceptions (Kim et al., 2021). Future research could greatly enhance the accuracy of results by capturing self-collected SVIs (Rui, 2023b). On other hand, this research derived the intensity of BSV by fitting the origin-destination points of bicycle-sharing data with the street network and identifying the shortest path. We calculated BSV based on communities, even though the deviation was almost negligible, we did not consider the diversity of path choices made by cyclists. Further research could acquire actual trajectory data to improve accuracy.

CRediT authorship contribution statement

Jin Rui: Writing – review & editing, Writing – original draft, Visualization, Validation, Supervision, Software, Resources, Project administration, Methodology, Investigation, Funding acquisition, Formal analysis, Data curation, Conceptualization. **Yuhan Xu:** Writing – original draft, Visualization, Software, Methodology, Formal analysis, Writing – review & editing.

Declaration of competing interest

The authors declare that they have no known competing financial interests or personal relationships that could have appeared to influence the work reported in this paper.

Data availability

Data will be made available on request.

Acknowledgements

We would like to extend our sincere gratitude to all the participants who took part in our study on rating the streetscape environment in March 2023. Your valuable insights and contributions have greatly enriched our research. We are thankful for the time and effort you dedicated to this project.

Appendix A. Descriptive analysis of dependent variables

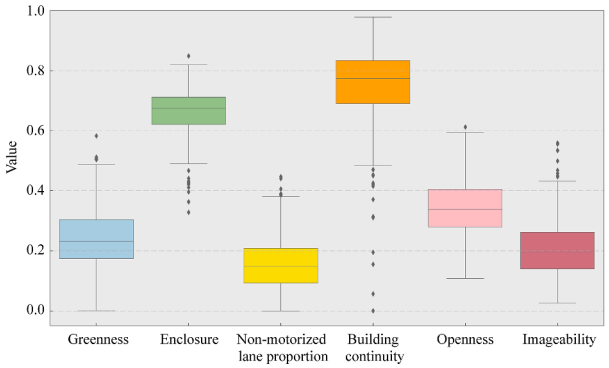

a. Boxplot of objective features

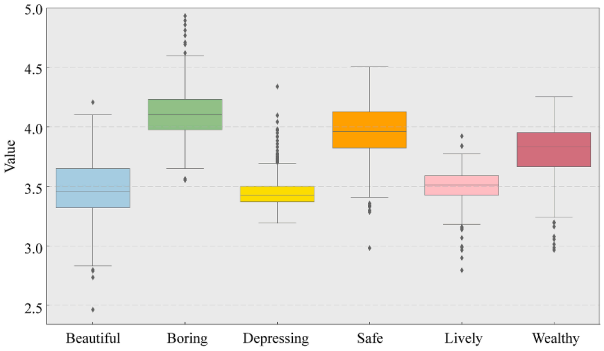

b. Boxplot of subjective perceptions

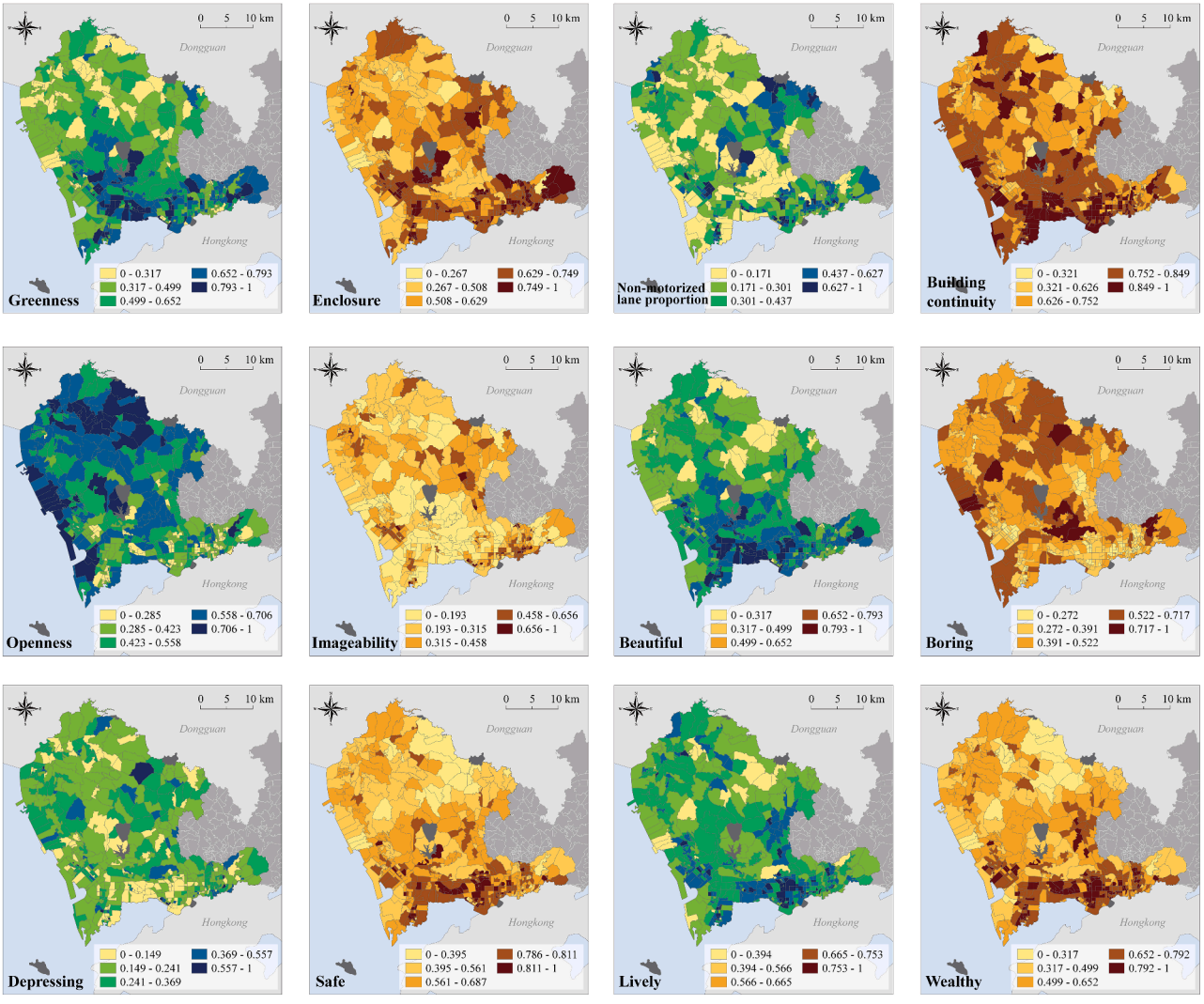

c. The spatial distributions of values of objective features and subjective perceptions in the study area.

Fig. A1. Boxplot and spatial distribution of values of objective features and subjective perceptions in the study area.

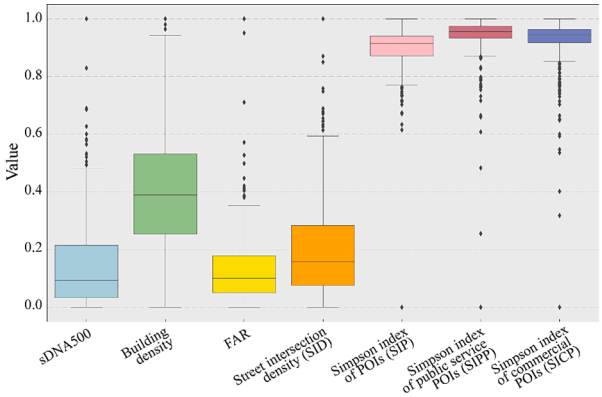

a. Boxplot of BE features

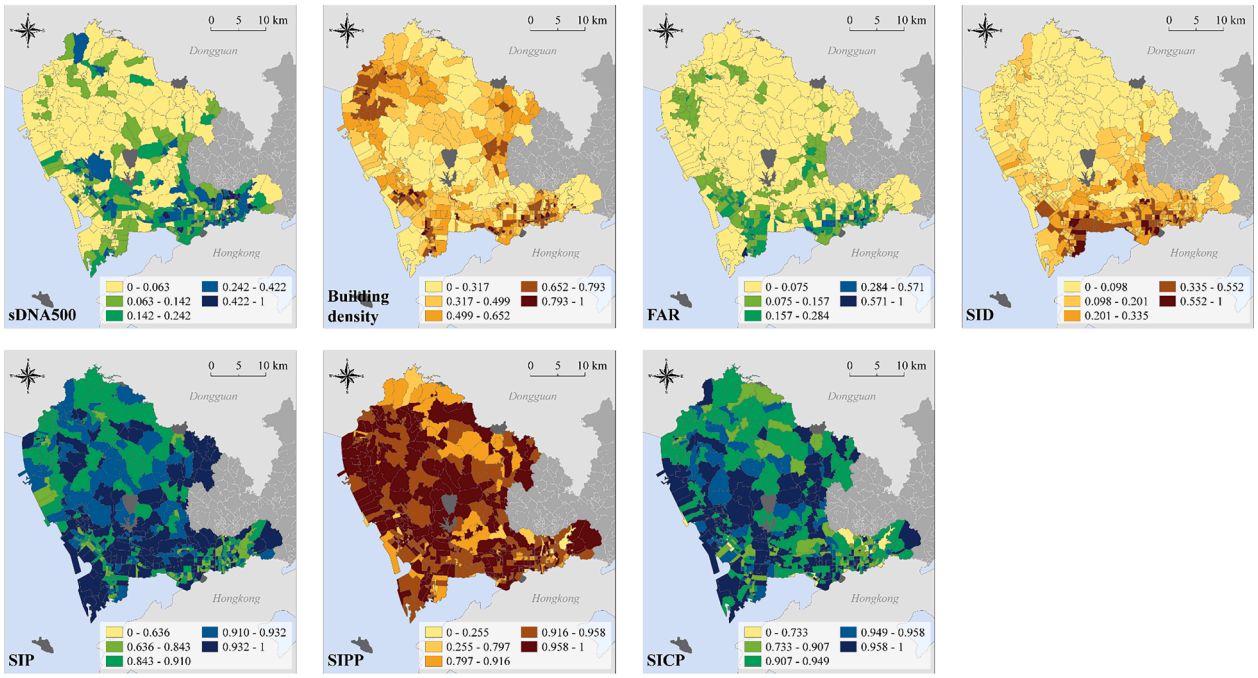

b. The spatial distributions of values of BE features in the study area.

Fig. A2. Boxplot and spatial distribution of values of BE features in the study area.

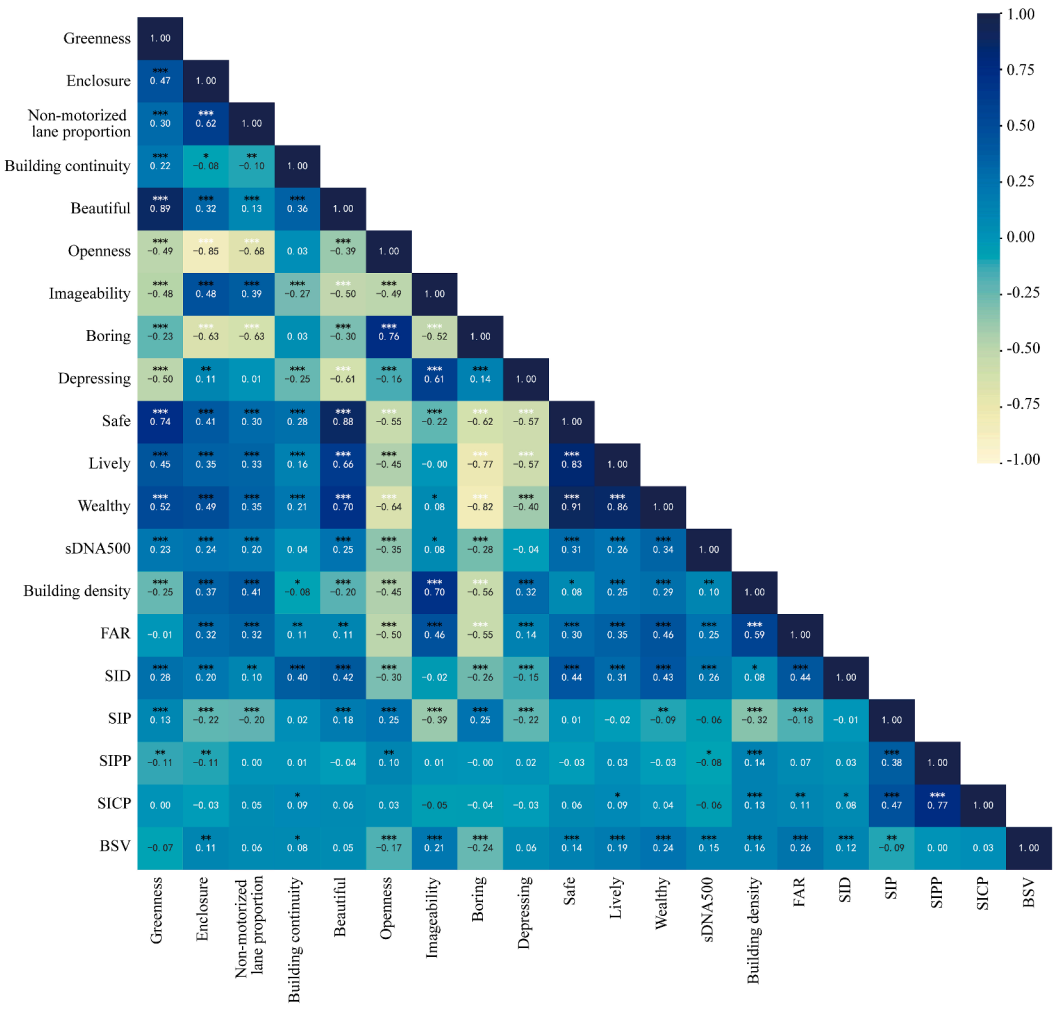

Fig. A3. Pearson correlations of all variables. **. p <0.01. **. p <0.05. *. p<0.1.

Appendix B. Tables

Table A
1 Comparison of different machine learning model performance.

	MSE		RMSE		MAE		MAPE	
	Train dataset	Test dataset	Train dataset	Test dataset	Train dataset	Test dataset	Train dataset	Test dataset
Decision tree	0.002	0.058	0.05	0.241	0.038	0.167	45.689	126.385
Radom forest	0.003	0.028	0.055	0.167	0.04	0.116	35.586	80.3
K-nearest neighbors	0.013	0.027	0.114	0.166	0.078	0.113	60.413	85.232
Support vector machines	0.016	0.025	0.127	0.159	0.085	0.101	68.187	72.913
LightGBM	0	0.027	0.022	0.164	0.009	0.114	15.939	87.791
Backpropagation	0.016	0.025	0.128	0.159	0.087	0.105	67.563	72.893
XGBoost	**0**	**0.023**	**0.001**	**0.154**	**0.001**	**0.116**	**4.81**	**71.118**

Table A
2 Descriptive statistics of all variables (n=481).

Variables	Max.	Min.	Mean.	S.D.
Greenness	0.583	0	0.244	0.097
Enclosure	0.849	0.328	0.664	0.074
Non-motorized lane proportion	0.447	0	0.158	0.086
Building continuity	0.979	0	0.749	0.127

(*continued on next page*)

Table A (*continued*)

Variables	Max.	Min.	Mean.	S.D.
Beautiful	4.208	2.463	3.473	0.242
Openness	0.612	0.108	0.341	0.09
Imageability	0.559	0.026	0.209	0.094
Boring	4.934	3.553	4.115	0.201
Depressing	4.34	3.19	3.454	0.139
Safe	4.505	2.981	3.962	0.229
Lively	3.923	2.795	3.499	0.138
Wealthy	4.253	2.965	3.801	0.224
sDNA500	13.234	0.075	1.977	1.916
Building density	16.782	0.001	2.158	1.908
FAR	2098.263	16.299	434.515	336.735
Street intersection density	0.813	0	0.729	0.06
Simpson index of POIs	0.94	0	0.877	0.108
Simpson index of public service POIs	0.933	0	0.854	0.117
Simpson index of commercial POIs	3984.085	0.127	546.984	579,586

Table A
3 Global Moran's I and z-score and p-value.

Variables selected	Global Moran's I Index	z-value	p-value
Bicycle-sharing intensity	0.413	18.915	<0.001
Greenness	0.410	18.642	<0.001
Enclosure	0.446	20.290	<0.001
Non-motorized lane proportion	0.243	11.095	<0.001
Building continuity	0.195	8.940	<0.001
Openness	0.544	24.673	<0.001
Imageability	0.236	10.763	<0.001
Beautiful	0.457	20.760	<0.001
Boring	0.424	19.292	<0.001
Depressing	0.072	3.362	<0.001
Safe	0.473	21.502	<0.001
Lively	0.378	17.250	<0.001
Wealthy	0.510	23.187	<0.001
sDNA500	0.370	16.924	<0.001
Building density	0.295	13.425	<0.001
FAR	0.340	15.711	<0.001
SID	0.481	21.884	<0.001
SIP	0.133	6.443	<0.001
SIPP	0.130	6.278	<0.001
SICP	0.151	7.183	<0.001

References

Brunsdon, C., Fotheringham, A. S., & Charlton, M. E. (1996). Geographically weighted regression: A method for exploring spatial nonstationarity. *Geographical Analysis, 28* (4), 281–298. https://doi.org/10.1111/j.1538-4632.1996.tb00936.x

Chen, T., & Guestrin, C. (2016). Xgboost: A scalable tree boosting system. In *Proceedings of the 22nd ACM SIGKDD international conference on knowledge discovery and data mining* (pp. 785–794).

De Nazelle, A., Nieuwenhuijsen, M. J., Antó, J. M., Brauer, M., Briggs, D., Braun-Fahrlander, C., Cavill, N., Cooper, A. R., Desqueyroux, H., & Fruin, S. (2011). Improving health through policies that promote active travel: A review of evidence to support integrated health impact assessment. *Environment International, 37*(4), 766–777. https://doi.org/10.1016/j.envint.2011.02.003

Dong, L., Jiang, H., Li, W., Qiu, B., Wang, H., & Qiu, W. (2023). Assessing impacts of objective features and subjective perceptions of street environment on running amount: A case study of Boston. *Landscape and Urban Planning, 235*, Article 104756. https://doi.org/10.1016/j.landurbplan.2023.104756

Ewing, R., & Handy, S. (2009). Measuring the unmeasurable: Urban design qualities related to walkability. *Journal of Urban design, 14*(1), 65–84. https://doi.org/10.1080/13574800802451155

Fan, Y., & Zheng, S. (2020). Dockless bike sharing alleviates road congestion by complementing subway travel: Evidence from Beijing. *Cities, 107*, Article 102895. https://doi.org/10.1016/j.cities.2020.102895

Fotheringham, A. S., Yang, W., & Kang, W. (2017). Multiscale geographically weighted regression (MGWR). *Annals of the American Association of Geographers, 107*(6), 1247–1265. https://doi.org/10.1080/24694452.2017.1352480

Gong, W., Rui, J., & Li, T. (2024). Deciphering urban bike-sharing patterns: An in-depth analysis of natural environment and visual quality in New York's Citi bike system. *Journal of Transport Geography, 115*, Article 103799. https://doi.org/10.1016/j.jtrangeo.2024.103799

Greenwell, B. M. (2017). pdp: An R Package for constructing partial dependence plots. *The R Journal, 9*(1), 421. https://doi.org/10.32614/RJ-2017-016

Haustein, S., Thorhauge, M., & Cherchi, E. (2018). Commuters' attitudes and norms related to travel time and punctuality: A psychographic segmentation to reduce congestion. *Travel Behaviour and Society, 12*, 41–50. https://doi.org/10.1016/j.tbs.2018.04.001

Hillier, B., & Hanson, J. (1989). *The social logic of space*. Cambridge university press.

Huang, W., Guo, Y., Guo, C., Tang, F., Zhao, Y., Xia, Z., & Zhang, R. (2023). Simulation of urban non-motorized traffic: A agent-based modeling approach based on big data of bike sharing and social force model. *Transactions in Urban Data, Science, and Technology, 2*(4), 204–222. https://doi.org/10.1177/27541231231180989

Ito, K., & Biljecki, F. (2021). Assessing bikeability with street view imagery and computer vision. *Transportation research part C: emerging technologies, 132*, Article 103371. https://doi.org/10.1016/j.trc.2021.103371

Kabisch, N., Pueffel, C., Masztalerz, O., Hemmerling, J., & Kraemer, R. (2021). Physiological and psychological effects of visits to different urban green and street environments in older people: A field experiment in a dense inner-city area. *Landscape and Urban Planning, 207*, Article 103998. https://doi.org/10.1016/j.landurbplan.2020.103998

Kim, J.-I., Yu, C.-Y., & Woo, A. (2023). The impacts of visual street environments on obesity: The mediating role of walking behaviors. *Journal of Transport Geography, 109*, Article 103593. https://doi.org/10.1016/j.jtrangeo.2023.103593

Kim, J. H., Lee, S., Hipp, J. R., & Ki, D. (2021). Decoding urban landscapes: Google street view and measurement sensitivity. *Computers, Environment and Urban Systems, 88*, Article 101626.

Li, Y., Liu, H., Lyu, C., Yang, N., & Liu, Z. (2023). Predicting of motor vehicle carbon emissions and spatio-temporal characteristic analysis in the Beijing-Tianjin-Hebei region. *Environmental Science and Pollution Research, 30*(18), 52717–52731. https://doi.org/10.1007/s11356-023-26035-z

Lin, D., Zhang, Y., & Meng, L. (2023). Assessing bike accessibility to metro systems by integrating crowdedness. *Transactions in Urban Data, Science, and Technology*. https://doi.org/10.1177/27541231231179403, 27541231231179403.

Lin, P., Weng, J., Liang, Q., Alivanistos, D., & Ma, S. (2020). Impact of weather conditions and built environment on public bikesharing trips in Beijing. *Networks and Spatial Economics, 20*, 1–17. https://doi.org/10.1007/s11067-019-09465-6

Lynch, K. (1964). *The image of the city*. MIT press.

Ma, X., Ma, C., Wu, C., Xi, Y., Yang, R., Peng, N., Zhang, C., & Ren, F. (2021). Measuring human perceptions of streetscapes to better inform urban renewal: A perspective of scene semantic parsing. *Cities, 110*, Article 103086. https://doi.org/10.1016/j.cities.2020.103086

Meng, M., Zhang, J., Wong, Y. D., & Au, P. H. (2016). Effect of weather conditions and weather forecast on cycling travel behavior in Singapore. *International Journal of Sustainable Transportation, 10*(9), 773–780. https://doi.org/10.1080/15568318.2016.1149646

Milakis, D., Gebhardt, L., Ehebrecht, D., & Lenz, B. (2020). Is micro-mobility sustainable? An overview of implications for accessibility, air pollution, safety, physical activity and subjective wellbeing. *Handbook of Sustainable Transport, 180*. https://doi.org/10.4337/9781789900477.00030

Moran, P. A. (1950). Notes on continuous stochastic phenomena. *Biometrika, 37*(1/2), 17–23.

Nawrath, M., Kowarik, I., & Fischer, L. K. (2019). The influence of green streets on cycling behavior in European cities. *Landscape and urban Planning, 190*, Article 103598. https://doi.org/10.1016/j.landurbplan.2019.103598

Niu, Z., & Chai, L. (2022). Carbon emission reduction by bicycle-sharing in China. *Energies, 15*(14), 5136. https://doi.org/10.3390/en15145136

Parkin, J., Wardman, M., & Page, M. (2008). Estimation of the determinants of bicycle mode share for the journey to work using census data. *Transportation, 35*, 93–109. https://doi.org/10.1007/s11116-007-9137-5

Pettersson, I., Hagberg, L., Fredriksson, C., & Hermansson, L. N. (2016). The effect of powered scooters on activity, participation and quality of life in elderly users. *Disability and Rehabilitation: Assistive Technology, 11*(7), 558–563. https://doi.org/10.3109/17483107.2015.1027301

Qiu, W., Li, W., Liu, X., Zhang, Z., Li, X., & Huang, X. (2023). Subjective and objective measures of streetscape perceptions: Relationships with property value in Shanghai. *Cities, 132*, Article 104037. https://doi.org/10.1016/j.cities.2022.104037

Rogers, W. P., III, Chen, N., & Looye, J. W. (2023). Beyond traditional TOD: Integrating multiuse paths and bike share into public transit to address the first/last mile issue. *Urban Rail Transit, 9*(1), 42–56. https://doi.org/10.1007/s40864-022-00182-x

Rui, J. (2023a). Exploring the association between the settlement environment and residents' positive sentiments in urban villages and formal settlements in Shenzhen. *Sustainable Cities and Society*. , Article 104851. https://doi.org/10.1016/j.scs.2023.104851

Rui, J. (2023b). Measuring streetscape perceptions from driveways and sidewalks to inform pedestrian-oriented street renewal in Düsseldorf. *Cities, 141*, Article 104472.

Rui, J., & Li, X. (2023). Decoding vibrant neighborhoods: Disparities between formal neighborhoods and urban villages in eye-level perceptions and physical environment. *Sustainable Cities and Society*, Article 105122.

Rui, J., Othengrafen, F., 2023, Examining the role of innovative streets in enhancing urban mobility and livability for sustainable urban transition: A review, *Sustainability* 15(7):5709. https://doi.org/10.3390/su15075709.

Shaaban, K., 2020, Why don't people ride bicycles in high-income developing countries, and can bike-sharing be the solution? The case of Qatar, *Sustainability* 12(4):1693. https://doi.org/10.3390/su12041693.

Shenzhen City Planning and Land Development Research Center. (2021). *Main conclusions of the seventh resident travel survey in Shenzhen*.

Shenzhen Municipal Bureau of Planning and Natural Resources, 2019, Shenzhen's '13th five-year' urban renewal plan.

Shenzhen Municipal Planning and Natural Resources Bureau, 2023, Territorial spatial planning of Nanshan District, Shenzhen. http://pnr.sz.gov.cn/attachment/1/1286/1286906/10543075.pdf.

Shenzhen Transportation Department. (2021). *Shenzhen bicycle transportation development plan (2021-2025)*.

Song, Q., Li, W., Li, J., Wei, X., & Qiu, W. (2023). Disclosing the impact of micro-level environmental characteristics on dockless bikeshare trip volume: A case study of ithaca. In *International conference on computers in urban planning and urban management* (pp. 125–147). Springer.

Spotswood, F., Chatterton, T., Tapp, A., & Williams, D. J. (2015). Analysing cycling as a social practice: An empirical grounding for behaviour change. *Transportation Research Part F: Traffic Psychology and Behaviour, 29*, 22–33. https://doi.org/10.1016/j.trf.2014.12.001

Su, Y., Wu, J., Ciais, P., Zheng, B., Wang, Y., Chen, X., Li, X., Li, Y., Wang, Y., & Wang, C. (2022). Differential impacts of urbanization characteristics on city-level carbon emissions from passenger transport on road: Evidence from 360 cities in China. *Building and Environment, 219*, Article 109165. https://doi.org/10.1016/j.buildenv.2022.109165

Thaler, U. (2020). Space syntax methodology. *Archaeological spatial analysis*, 296–312.

Tong, Z., Zhu, Y., Zhang, Z., An, R., Liu, Y., & Zheng, M. (2023). Unravel the spatio-temporal patterns and their nonlinear relationship with correlates of dockless shared bikes near metro stations. *Geo-spatial Information Science, 26*(3), 577–598.

Wang, C., & Zhang, Y. (2023). Inferring and comparing trip purposes of shared micromobility services: A case study of Ningbo, China. *Transactions in Urban Data, Science, and Technology*. https://doi.org/10.1177/27541231231179884, 27541231231179884.

Wang, L., Han, X., He, J., & Jung, T. (2022). Measuring residents' perceptions of city streets to inform better street planning through deep learning and space syntax. *ISPRS Journal of Photogrammetry and Remote Sensing, 190*, 215–230. https://doi.org/10.1016/j.isprsjprs.2022.06.011

Wu, C., Ye, Y., Gao, F., & Ye, X. (2023). Using street view images to examine the association between human perceptions of locale and urban vitality in Shenzhen, China. *Sustainable Cities and Society, 88*, Article 104291. https://doi.org/10.1016/j.scs.2022.104291

Zhang, F., Zhou, B., Liu, L., Liu, Y., Fung, H. H., Lin, H., & Ratti, C. (2018). Measuring human perceptions of a large-scale urban region using machine learning. *Landscape and Urban Planning, 180*, 148–160. https://doi.org/10.1016/j.landurbplan.2018.08.020